



LAWRENCE  
LIVERMORE  
NATIONAL  
LABORATORY

LLNL-PROC-838374

# Radiation Hardness of Polycrystalline Ceramic Scintillators for Radioisotope Batteries

J. T. Jarrell, N. J. Cherepy, Z. M. Seeley, E. L. Swanberg, L. F. Voss, M. A. Stoyer, R. A. Henderson, R. J. Nikolic

August 2, 2022

SPIE Optical Engineering and Applications  
San Diego, CA, United States  
August 21, 2022 through August 25, 2022

## **Disclaimer**

---

This document was prepared as an account of work sponsored by an agency of the United States government. Neither the United States government nor Lawrence Livermore National Security, LLC, nor any of their employees makes any warranty, expressed or implied, or assumes any legal liability or responsibility for the accuracy, completeness, or usefulness of any information, apparatus, product, or process disclosed, or represents that its use would not infringe privately owned rights. Reference herein to any specific commercial product, process, or service by trade name, trademark, manufacturer, or otherwise does not necessarily constitute or imply its endorsement, recommendation, or favoring by the United States government or Lawrence Livermore National Security, LLC. The views and opinions of authors expressed herein do not necessarily state or reflect those of the United States government or Lawrence Livermore National Security, LLC, and shall not be used for advertising or product endorsement purposes.

# Radiation hardness of polycrystalline ceramic scintillators for radioisotope batteries

Joshua T. Jarrell<sup>\*a</sup>, Nerine Cherepy<sup>a</sup>, Zachary Seeley<sup>a</sup>, Erik Swanberg<sup>a</sup>, Lars Voss<sup>a</sup>, Clint Frye<sup>a</sup>, Mark Stoyer<sup>a</sup>, Roger Henderson<sup>a</sup>, Rebecca Nikolic<sup>a</sup>

<sup>a</sup>Lawrence Livermore National Laboratory, CA, USA 94550

## ABSTRACT

The usefulness of GYGAG(Ce) transparent polycrystalline ceramic garnet scintillators as the conversion medium in alpha and beta-fueled radioisotope batteries was explored through alpha irradiations and 0.5-2 MeV electron irradiations. Absorption spectra and light yields were measured before and after irradiations. Within experimental error no degradation in light yield was observed for the electron-irradiated samples as measured via beta or gamma excitation. A small increase in optical absorption near the emission wavelength was observed following the largest dose irradiation. Significant reduction in light yield was observed following helium ion irradiation. Partial recovery of the light yield was observed following annealing in oxygen above 400°C for helium ion irradiated samples. These results suggest that GYGAG(Ce) may prove useful for beta-fueled scintillation-based radioisotope batteries by allowing for higher energy beta emitters, increased power densities, and long service lifetimes.

**Keywords:** Alpha particles, beta particles, nuclear batteries, radiation hardness, transparent ceramics, scintillation, thermal annealing

## 1. INTRODUCTION

Radioisotope batteries rely on the conversion of nuclear decay energy into electricity to perform useful work. Methods of conversion include direct and indirect transfer of ionizing radiation energy into electricity. For direct energy conversion, the ionizing energy is converted into electricity through the liberation and collection of electrons or charged ions. For indirect conversion, the energy of the ionizing radiation resultant from radioactive decay is first converted into a second form, such as light in the case of scintillator-based conversion schemes, or heat in the case of thermal conversion such as that found in radioisotope thermoelectric generators (RTGs)<sup>1</sup>.

The conversion of the kinetic energy of ionizing radiation into electricity possesses the highest theoretical efficiency in the case of direct conversion schemes. This is unsurprising, since a more direct conversion process will intrinsically have fewer transmutations, each with its own sub-unity efficiency. Alpha and betavoltaics make use of a direct conversion mechanism to achieve high power density but the conversion medium, a semiconductor substrate, suffers cumulative radiation damage which leads to degradation of the converter unless very low energy radiation, on the order of less than 100 keV is used<sup>2</sup>. However, to achieve high power densities in radioisotope batteries, radiation with energies in the range of hundreds of keV to several MeV is preferred<sup>3,4</sup>. This limits the materials which can be used in direct conversion schemes. In contrast, indirect conversion schemes intrinsically are less efficient when compared to ideal direct conversion methods, but the materials used often possess greater radiation hardness and are more tolerant to radiation induced defects<sup>5,6</sup>.

Two methods of indirect conversion include thermoelectric conversion and scintillation. In the former case, as demonstrated by the success of RTGs which are well suited to generating hundreds of watts of electrical power, the required conversion medium can operate for decades without significant degradation<sup>7</sup>. However, thermal conversion schemes are difficult to scale down to the milliwatt range, due largely to difficulties maintaining a sufficient temperature gradient to extract usable power. In contrast, scintillation-based radioisotope batteries rely on the conversion of the kinetic energy of ionizing radiation into photons, which are then converted into electricity, commonly by photovoltaic cells. This decouples the relatively sensitive photovoltaic cells from the ionizing radiation, but many common scintillator materials are damaged by low energy radiation in the range of a few hundred keV<sup>1</sup>.

In this investigation, the radiation hardness of a polycrystalline ceramic, GYGAG(Ce), was explored by irradiation of the scintillators by <sup>210</sup>Po alpha particles, accelerated helium ions in the energy range of 1 to 4 MeV, and accelerated electrons

in the energy range of 0.5 to 2 MeV. The investigation included measurement of light yield degradation under alpha, beta, and gamma excitation, changes in the optical absorption spectrum, and recovery of light yield by thermal annealing.

## 2. CHARACTERIZATION OF TRANSPARENT POLYCRYSTALLINE CERAMIC SCINTILLATORS

The development of polycrystalline ceramic scintillators has introduced a class of radiation-hard scintillators which emit photons in the visible spectrum with relatively high light yields<sup>8,9</sup>. Examples of such scintillators and related materials include polycrystalline YAG:Ce, BGO, LuAG, and LYSO.GYGAG(Ce)<sup>10</sup>. Significant radiation hardness studies have been performed on these materials, primarily focused on the effects of proton and heavy ion irradiation<sup>10-12</sup>.  $\text{Gd}_{1.5}\text{Y}_{1.5}\text{Ga}_{2.2}\text{Al}_{2.8}\text{O}_{12}(\text{Ce})$ , is a transparent polycrystalline scintillator activated with cerium which emits light in the range of 450-700 nm, centered around approximately 550 nm. The typical light yield for sintered GYGAG(Ce) produced from sintered and hot pressing of nanoparticles is approximately 50 photons/keV. The density and effective Z of GYGAG(Ce) are 5.8 g/cm<sup>3</sup> and 48, respectively<sup>13</sup>.

To investigate the effects of radiation on the scintillators, several samples were prepared by the hot press sintering process as described by Cherepy et al<sup>13</sup>. Sample thicknesses ranged from 5mm for the electron irradiated samples to a minimum thickness of 200  $\mu\text{m}$  for the alpha and helium ion irradiated samples. A constant diameter of 18 mm the samples was used for all samples. Figure 1 and Figure 2 show the optically polished and thinned sample and 5 mm samples, respectively.

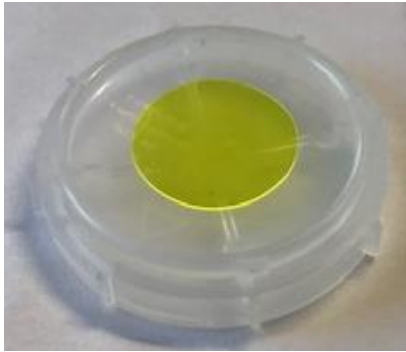


Figure 1. A thinned and optically polished GYGAG(Ce) sample used in the alpha irradiation experiments<sup>14</sup>.

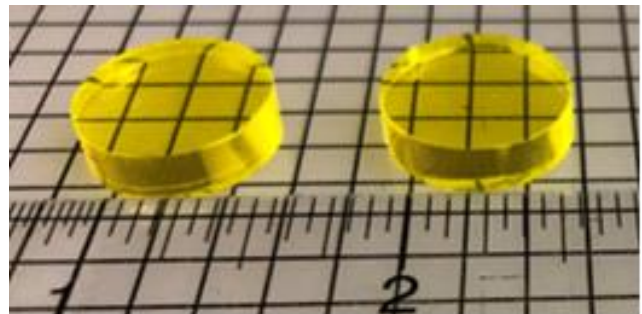


Figure 2. Several of the unirradiated transparent GYGAG(Ce) samples used in the electron irradiation experiment<sup>14</sup>.

The radioluminescent emission spectra and light yield from the scintillator samples were collected before and after irradiation using a Princeton Instruments/Acton Spec 10 spectrograph coupled to a thermoelectrically cooled CCD camera. Alpha particles from a <sup>210</sup>Po source with a maximum range of approximately 10  $\mu\text{m}$  were used as the excitation source to probe the surface for radiation damage. Beta particles from a <sup>90</sup>Sr/<sup>90</sup>Y source were used to probe the volume of each sample irradiated by electrons. The endpoint energy of the <sup>90</sup>Sr/<sup>90</sup>Y source is well matched with the maximum energy of 2 MeV used in the electron irradiations. Gamma particles with a half-value layer thickness of 15.5mm in the scintillators from a <sup>137</sup>Cs source were used to uniformly stimulate the full volume of each electron-irradiated sample. The scintillation pulse height spectra were acquired using a 2" Hamamatsu R6231-100 PMT. These signals were shaped using a Tennelec TC 244 spectroscopy amplifier and recorded using an Amptek MCA8000-A multichannel analyzer. The full width half max (FWHM) of the scintillators was compared to unirradiated samples to determine the change in resolution of the samples.

In the case of the helium ion irradiated samples, thermal annealing at several temperatures was performed to observe the recovery of light yield as a function of isochronal annealing in air. By heating the scintillating material, some amount of

diffusion of defects can be annealed out of the material. For beta and gamma irradiation, this consists of the removal of color centers by supplying sufficient thermal energy to the trapped charge, recombination of vacancy and interstitial defect pairs, and the formation of neutral defect complexes<sup>14-16</sup>. Similar recovery can be observed in alpha and heavy ion irradiated material along the pathlength of the particles, where the introduced vacancies and interstitials can recombine. It is theorized that the polycrystalline microstructure of ceramic scintillators aids in the damage recovery by providing defect sinks and facilitating oxygen diffusion at the grain boundaries<sup>9</sup>.

### 3. RADIATION DAMAGE IN GYGAG(CE)

Scintillator samples were irradiated using alpha particles from  $^{210}\text{Po}$  decay, accelerated helium ions, and electrons. Particle fluences for the accelerated ions and electrons were chosen based on the cumulative fluence a mW-scale radioisotope battery would accumulate over ten years of operation. Particle fluxes were chosen to reduce the total irradiation time to a practical timeframe for accelerator operation, on the order of hours to a few days. Adequate sample cooling was then required to mitigate sample temperature rise because of the energy deposited by the incident flux of particles.

#### 3.1 $^{210}\text{Po}$ alpha particle irradiation of GYGAG(Ce)

A scintillator sample was placed on an approximately 4.2 mCi commercial NucleSpot  $^{210}\text{Po}$  alpha source in air. The  $^{210}\text{Po}$  source consists of a thin plate of  $^{210}\text{Po}$  recessed approximately 3 mm from the housing surface. The alpha particles escape through an 18 mm diameter window. The alpha-stimulated light yield of the sample was measured as described above. After measuring the light yield, the GYGAG(Ce) sample remained on the  $^{210}\text{Po}$  source for 62 days to accumulate a total fluence of approximately  $5 \times 10^{13}/\text{cm}^2$  estimated using MCNP6 Monte Carlo simulations.

The scintillator sample irradiated for approximately 63 days under a  $^{210}\text{Po}$  source showed no degradation in light yield within the measurement error. The decreasing light output from the  $^{210}\text{Po}$  irradiated sample follows the expected decay from  $^{210}\text{Po}$ , decaying with a half-life of 138.4 days to within 5% at each measurement. The sample was briefly removed and reinstalled on day 62, resulting in a larger than expected deviation due to a slight geometry change. The decreasing light yield over time and emission spectra for the sample irradiated to a fluence of  $5 \times 10^{13}/\text{cm}^2$  with a  $^{210}\text{Po}$  source are shown in Figure 3 and Figure 4, respectively. No change in optical absorption was observed for the sample irradiated by  $^{210}\text{Po}$  to a fluence of approximately  $5 \times 10^{13}/\text{cm}^2$ .

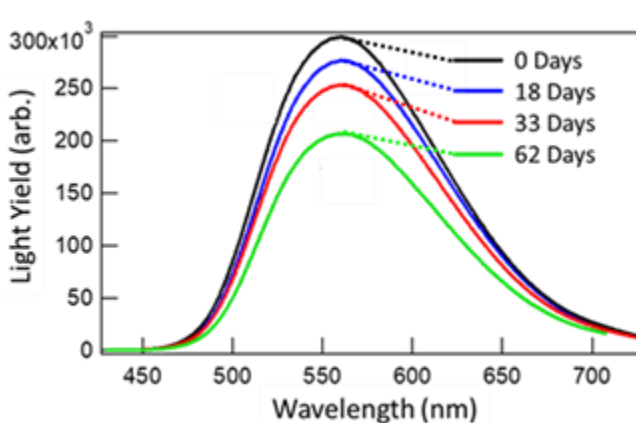


Figure 3. Quantitative alpha radioluminescence of GYGAG(Ce) sample over time. The decreasing light yield follows the half-life of the  $^{210}\text{Po}$  source.

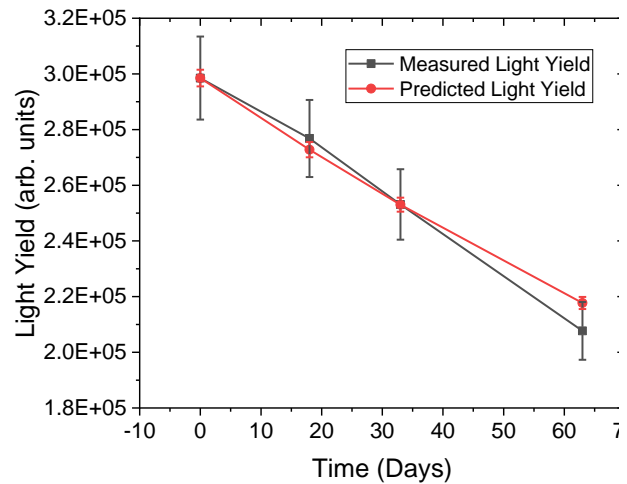


Figure 4. Measured and predicted change in light yield over the exposure time for the  $^{210}\text{Po}$  irradiated GYGAG(Ce) sample.

### 3.2 Helium ion irradiation of GYGAG(Ce)

An optically polished and thinned GYGAG(Ce) sample was irradiated to a total fluence of  $10^{16}/\text{cm}^2$  with ionized helium nuclei at the Nanoscale Integration Science laboratory of Lawrence Livermore National Laboratory. The accelerator used is a 4 MV Van de Graaff generator capable of delivering an helium ion flux up to  $10^{14}/\text{cm}^2\text{-sec}$ . The target was mounted on a thermally and electrically conductive copper finger in vacuum and held at approximately 300K. The sample was mounted on the finger using conductive silver paint to maintain the temperature and avoid electrostatic charge buildup. The GYGAG(Ce) sample was irradiated at a flux of  $10^{12}/\text{cm}^2\text{-sec}$  with a rastered beam to ensure that the dose was uniform across the sample. The fluence was divided evenly between seven energies equally spaced from 0.5 to 3.5 MeV. The energy was varied to simulate the energy distribution of an isotropically radiating source on the surface of the GYGAG(Ce) sample. The maximum range of a 3.5 MeV helium nucleus in the GYGAG(Ce) sample was calculated using SRIM-2013 to be approximately 10  $\mu\text{m}$ , thus the radiation damage was estimated to be concentrated in a 10  $\mu\text{m}$  deep region of the sample. After irradiation, the sample and copper finger were removed from the accelerator beamline. Acetone was used to dissolve the silver paint. The sample was then cleaned in a cleanroom facility ultrasonic bath with acetone, rinsed with isopropyl alcohol and deionized water, and dried with nitrogen. After cleaning, the sample was characterized using light yield and UV-Vis spectroscopic measurements.

The optical absorption spectrum of the scintillators was measured at room temperature before and after irradiation using a Thermo Evolution 220 UV-Vis spectrometer. As shown in Figure 5, the absorption to shorter wavelengths increased after ion beam irradiation<sup>14</sup>. The optical absorption around the emission wavelength of GYGAG(Ce), which is from approximately 450 to 700 nm, does not appreciably increase above 500 nm after irradiation. Color center formation is well-known for scintillators in the application of high-dose X-ray applications<sup>9</sup>. In contrast,

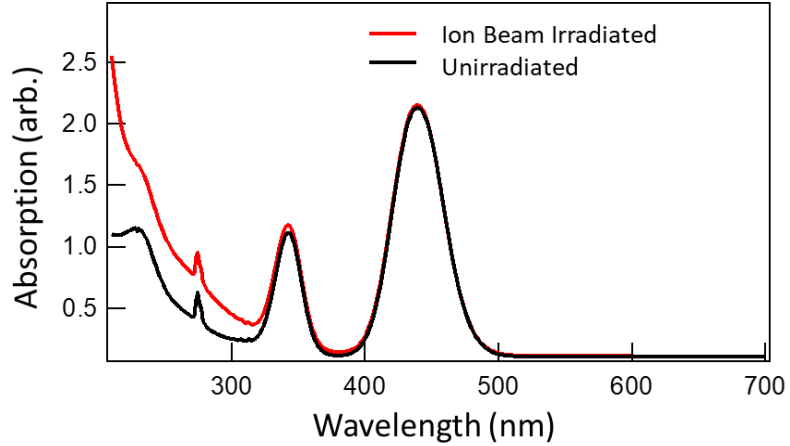


Figure 5. The optical absorption spectrum of a GYGAG(Ce) sample before and after irradiation by helium ions to a fluence of  $10^{16}/\text{cm}^2$ .

measurement of the light yield of the ion irradiated sample demonstrated the necessity to use a suitable excitation source. Given that the sample was 200  $\mu\text{m}$  thick and the helium ion range at 3.5 MeV is approximately 10  $\mu\text{m}$  in the sample material, the radiation damage accumulates near the surface of the sample. beta radioluminescence as a surrogate for the unirradiated response of the ion beam irradiated sample.

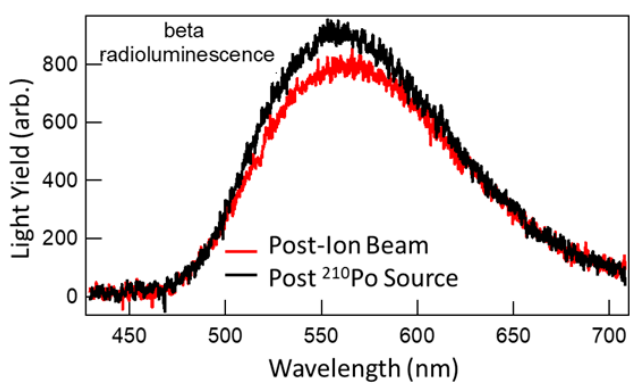


Figure 6. The beta-excited radioluminescence emission spectra for the ion irradiated sample and the  $^{210}\text{Po}$  irradiated sample. Only minimal degradation is detected using beta stimulated radioluminescence<sup>14</sup>.

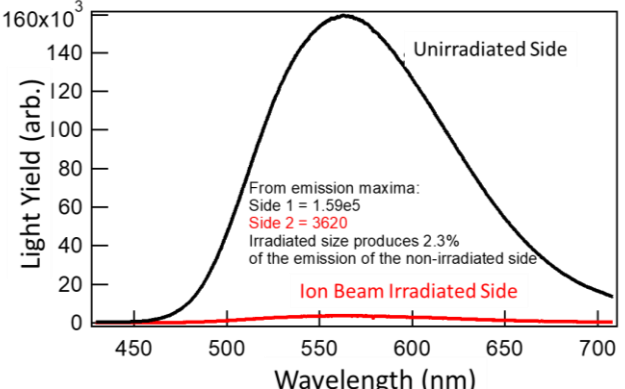


Figure 7. The alpha-excited radioluminescence emission spectra from the helium ion irradiated sample surface. Significant degradation is demonstrated, in contrast with the measurement using beta-excitation.

Following the beta excited emission measurement, the electron and helium irradiated samples were characterized for alpha light yield with the  $^{210}\text{Po}$  source. Figure 6 and Figure 7 show the light yield measurements before and after irradiation when the sample is excited by a  $^{90}\text{Sr}/^{90}\text{Y}$  beta source and a  $^{210}\text{Po}$  source, respectively. This probing method separates surface effects from bulk effects. Both sides of the GYGAG(Ce) samples were excited with the alpha source and the light yield measured separately for each side. The resulting light yield for the unirradiated and irradiated side of the GYGAG(Ce) sample is shown in Figure 7. The light yield for the helium ion irradiated sample decreased to 2.3% of the initial light yield following irradiation to a fluence of  $10^{16} \text{ ions}/\text{cm}^2$ . In Figure 6, the helium ion irradiated sample's beta radioluminescence spectrum is compared to that of the  $^{210}\text{Po}$  irradiated sample, which suffered no degradation.

### 3.3 Thermal annealing of ion irradiated GYGAG(Ce)

After the light yield and optical absorption measurements were performed on the helium irradiated GYGAG(Ce) sample, it was annealed at increasing temperatures in air. Following the ion beam irradiation, the sample was held at room temperature in air for 3 weeks, after which the light yield was measured. The sample was then annealed at elevated temperatures for set durations. The light yield was measured after each anneal and the cumulative percentage light yield recovered was calculated.

Each sample underwent isochronal anneals at multiple temperatures in an air atmosphere. After annealing, the samples were cooled, and the light yield and optical absorption spectra were recorded. The alpha-induced radioluminescence of the ion beam irradiated sample after 3 weeks at room temperature, 12 hours at 400°C, and 12 hours at 800°C is shown in Figure 8. Each plot shows the alpha-excited radioluminescence spectrum of the unirradiated and irradiated sides, respectively.

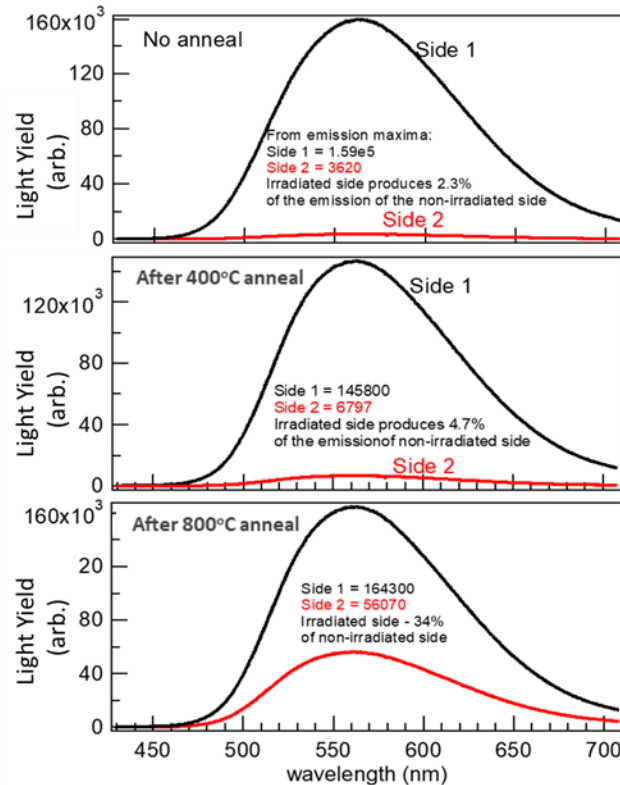


Figure 8. Cumulative recovery of light yield from alpha radioluminescence at various annealing temperatures. After 3 weeks of room temperature annealing (Top), 12 hours at 400°C, and 12 hours at 800°C.

The light yield recovery rate increases with increasing annealing temperature as seen in Figure 8. No recovery in light yield was observed over the 3-week room temperature anneal, while the annealing rate for the 800°C anneal was roughly 8-fold larger than for the 400°C anneal.

### 3.4 Electron irradiation of GYGAG(Ce)

As has been previously discussed, electron irradiations were performed on GYGAG(Ce) samples in the energy range of 0.5 MeV to 2 MeV to fluences ranging from  $2 \times 10^{12}$  e<sup>-</sup>/cm<sup>2</sup> to  $10^{19}$  e<sup>-</sup>/cm<sup>2</sup><sup>14</sup>. As previously reported, the samples demonstrated no degradation in light yield within the measurement error, approximately 5%. Figure 9 shows the beta-excited emission spectrum for a sample irradiated with 0.75 MeV electrons to a fluence of  $10^{19}$  e<sup>-</sup>/cm<sup>2</sup>. Table 1 shows the measured change in light yield for each sample and the corresponding energy and fluence for the samples under beta excitation. This procedure was repeated using a <sup>210</sup>Po alpha source, the results of which are shown in Table 2. Due to the

sensitivity of the alpha excitation to surface preparation, the measurement error was significantly larger than that of the beta excitation measurements.

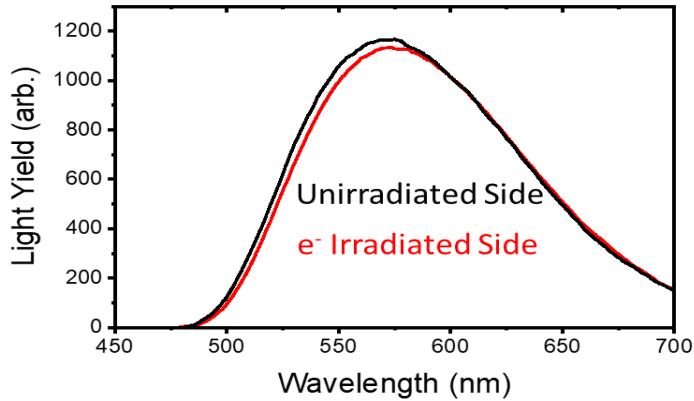


Figure 9. The beta-excited radioluminescence spectra from a GYGAG(Ce) sample after irradiation with 0.75 MeV electrons to a fluence of  $10^{19} \text{ e}/\text{cm}^2$ <sup>14</sup>

Table 1. Beta-Excited Light Yield As A Function Of Irradiation Energy And Fluence<sup>14</sup>

Energy (MeV)	$e^-$ Range (cm)	Fluence ( $\text{e}/\text{cm}^2$ )	$\Delta$ Light Yield (%)
0.5	0.06	$10^{17}$	$-8.0 \pm 8$
0.75	0.1	$10^{17}$	$-5.0 \pm 7$
0.75	0.1	$10^{19}$	$-3.5 \pm 7$
1.0	0.14	$10^{16}$	$0 \pm 5$
1.0	0.14	$10^{17}$	$-6.9 \pm 6$
2.0	0.30	$10^{17}$	$-0.4 \pm 5$

Table 2 Alpha-Excited Light Yield As A Function Of Irradiation Energy And Fluence<sup>14</sup>

Energy (MeV)	$e^-$ Range (cm)	Fluence ( $\text{e}/\text{cm}^2$ )	$\Delta$ Light Yield (%)
0.5	0.06	$10^{17}$	$-15.0 \pm 12$
0.75	0.1	$10^{17}$	$-11 \pm 11$
1.0	0.14	$10^{17}$	$-9.0 \pm 10$
2.0	0.30	$10^{17}$	$-9.0 \pm 10$

As in the case of the alpha and helium ion irradiated samples, optical absorption spectroscopy was performed. However, due to the greater thickness of the electron irradiated samples which prevented direct measurement of the optical absorption, the irradiated samples were first cut into 500  $\mu\text{m}$  thick samples, one from the irradiated surface and the other from the unirradiated surface of the sample. These samples were then measured and compared as shown in Figure 10<sup>14</sup>.

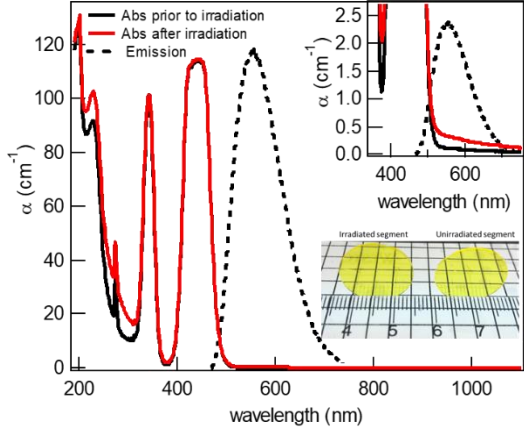


Figure 10. The electron irradiated GYGAG(Ce) optical absorption spectrum in terms of  $\alpha(\lambda)$  of the irradiated and unirradiated regions. For the sample irradiated by 0.75 MeV electrons to  $10^{19}$  e/cm<sup>2</sup>, a small increase in absorption exists in the emission wavelength range, shown above around 500 nm.

As is evident in Figure 10, a small increase in the parasitic absorption coefficient of  $0.20\text{ cm}^{-1}$  located in the emission wavelength range was generated by irradiation with 0.75 MeV electrons to a fluence of  $10^{19}$  e/cm<sup>2</sup>. This increase would lead to an absorption-induced light loss of approximately 1% in a  $500\text{ }\mu\text{m}$  thick sample, or approximately 63% of the unirradiated transmission for a 1 cm thick sample.

For a selection of the electron irradiated samples, the full volume of the sample was probed using a several microcurie  $^{137}\text{Cs}$  gamma source. The light yield and gamma spectroscopy performance of the GYGAG(Ce) sample irradiated with 0.75 MeV electrons to a fluence of  $10^{19}$  e/cm<sup>2</sup> was measured and is shown in Figure 11<sup>14</sup>. No degradation in the light yield is evident within the approximate 5% measurement error. However, the resolution of the gamma spectroscopy system is degraded from a typical resolution of 5% FWHM at the 662 keV photopeak to approximately 6% FWHM.

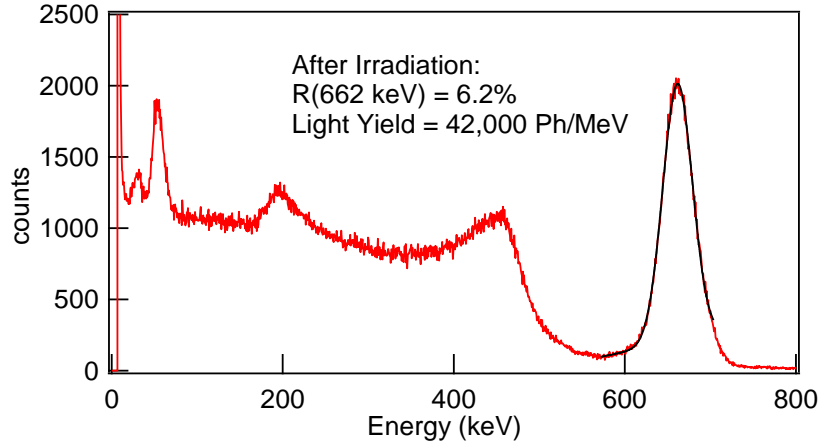


Figure 11. The  $^{137}\text{Cs}$  gamma spectrum measured using a GYGAG(Ce) sample irradiated to  $10^{19}$  e/cm<sup>2</sup> at 750 keV. The photoelectric peak has a resolution of ~6% and is consistent with a Gaussian distribution.

#### 4. DISCUSSION OF RESULTS

#### 4.1 Degradation mechanism in helium ion irradiated GYGAG(Ce)

As shown in the optical absorption spectra of Figure 11, the absorption to shorter wavelengths increases after helium irradiation to a fluence of  $10^{16}/\text{cm}^2$ , but not in the wavelengths of emission for the GYGAG(Ce) scintillation. This implies that a decrease in light yield from helium ion radiation damage may not predominantly be due to increased absorption in the emission wavelength. In contrast, after irradiation to a fluence of  $10^{16}/\text{cm}^2$ , the alpha-excited light yield is reduced to only 2.3% of the unirradiated light yield for the sample while the beta-excited emission is reduced by only approximately 10%. Since the beta particles from the  $^{90}\text{Sr}/^{90}\text{Y}$  source have a range greater than the damaged region of the scintillator, the full volume was excited which reduced the observed degradation. The degradation in light yield for alpha irradiation may be due to the clustering of defects near the end of the alpha trails, increasing the quenching effect on the scintillation or amorphization of the polycrystalline material. These results indicate that the useful environments for room temperature applications of GYGAG(Ce) scintillators should be limited to a fluence of less than  $10^{16}/\text{cm}^2$  of alpha particles to retain an appreciable light yield over the life of the scintillator.

#### 4.2 Annealing of helium ion-induced radiation damage

The annealing experiments confirm that the light yield can be appreciably recovered by annealing the irradiated scintillators in air at a temperature as low as  $400^\circ\text{C}$ , and the annealing rate rapidly increases with increasing annealing temperature up to at least  $800^\circ\text{C}$ . The lack of recovery from the room temperature anneal suggests that there is an associated thermal activation energy required, such as for re-crystallization of amorphized domains, and is consistent with the temperature of crystallization of the garnet, which is in the  $800\text{--}1000^\circ\text{C}$  range.

#### 4.3 Effects of electron irradiation on light yield and optical absorption

The GYGAG(Ce) samples irradiated with high energy electrons showed no measurable decrease in the light yield irrespective of fluence, energy, or dose when -excited by beta or gamma sources when measured with a system capable of approximately 5% error. This result indicates that the scintillating centers in the samples are unaffected by electron irradiation at the tested fluences and energies. A possible cause of the observed resilience to point defects, especially in the case of the  $10^{19}/\text{cm}^2$  irradiated sample, may be the migration of point defects to the grain boundaries at the irradiation temperatures which are above room temperature. However, from the alpha irradiation annealing experiments it is appears that annealing defect complexes capable of altering the light yield requires temperatures near  $400^\circ\text{C}$ , thus this is less likely for the lower fluence irradiations. Alternatively, the defect complexes which form may have minimal cross-section for absorption at the scintillation emission energy and do not therefore significantly degrade the light yield.

For the highest dose sample, which was irradiated using 750 keV electrons, the gamma spectroscopy resolution of the sample when measuring a  $^{137}\text{Cs}$  source was somewhat degraded from 5% to 6% FWHM at the 662 keV photopeak for irradiated samples and indicates that some material inhomogeneity in light yield was permanently introduced into the sample by irradiation.

### 5. SUMMARY

The radiation hardness of GYGAG(Ce) polycrystalline scintillators to alpha, helium ion, and electron irradiation has been explored in this work using light yield, optical absorption, and gamma spectroscopy techniques. Alpha irradiation from a  $^{210}\text{Po}$  source was found not to degrade the light yield of GYGAG(Ce), likely due to the small total fluence which can practically be applied by practical laboratory alpha sources. Helium ions were found to significantly degrade the light yield of GYGAG(Ce) scintillators at a fluence of  $10^{16}$  ions/ $\text{cm}^2$ . In contrast, no measurable degradation in light yield was detected within the measurement uncertainty for GYGAG(Ce) samples irradiated with electrons up to 2 MeV and  $10^{19}$  e<sup>-</sup>/ $\text{cm}^2$ , though a small increase in optical absorption in the emission spectrum was noted. These results imply that GYGAG(Ce) is not well suited to alpha-fueled scintillation radioisotope batteries. However, it may be useful as a scintillation conversion material for beta-fueled radioisotope batteries with beta endpoint energies of at least 2 MeV, such as is found in  $^{90}\text{Sr}/^{90}\text{Y}$  sources, provided that the GYGAG(Ce) thickness is minimized to limit attenuation through

absorption. The use of higher energy beta particles without degradation of the scintillator could provide increased power density and range of suitable radioisotopes in beta-fueled radioisotope batteries.

## REFERENCES

1. Prelas, M. *et al. Introduction to nuclear batteries and radioisotopes. Lecture Notes in Energy* vol. 56 (2016).
2. Bailey, S. G., Wilt, D. M., Castro, S. L., Cress, C. D. & Raffaelle, R. P. Photovoltaic development for alpha voltaic batteries. *Conf. Rec. IEEE Photovolt. Spec. Conf.* 106–109 (2005) doi:10.1109/pvsc.2005.1488080.
3. Shao, Q. *et al.* Radiation Hardness of Si Compared to 4H-SiC for Betavoltaics Assessed by Accelerated Aging Using an Electron Beam System. *J. Electron. Mater.* **51**, 350–355 (2022).
4. Xue, S. *et al.* Methods for improving the power conversion efficiency of nuclear-voltaic batteries. *Nucl. Instruments Methods Phys. Res. Sect. A Accel. Spectrometers, Detect. Assoc. Equip.* **927**, 133–139 (2019).
5. Schott, R. J. *et al.* Photon intermediate direct energy conversion using a 90Sr beta source. *Nucl. Technol.* **181**, 349–353 (2013).
6. Rensing, N. M. *et al.* Study of radiation damage in SrI<sub>2</sub> for 90Sr based betabatteries. *IEEE Nucl. Sci. Symp. Conf. Rec.* 1562–1566 (2011) doi:10.1109/NSSMIC.2011.6154632.
7. Landis, G. A. *et al.* Non-solar photovoltaics for small space missions. *Conf. Rec. IEEE Photovolt. Spec. Conf.* 2819–2824 (2012) doi:10.1109/PVSC.2012.6318178.
8. Lecoq, P., Gektin, A. & Korzhik, M. P. *Particle Acceleration and Detection Inorganic Scintillators for Detector Systems Physical Principles and Crystal Engineering.* (Springer, 2017).
9. Greskovich, C. & Duclos, S. Ceramic scintillators. *Annu. Rev. Mater. Sci.* **27**, 69–88 (1997).
10. Scintillators, P. W. O. C. *et al.* Proton-Induced Radiation Damage in BaF<sub>2</sub>, LYSO, . **65**, 1018–1024 (2018).
11. Hirouchi, T. *et al.* Effect of ion beam and neutron irradiations on the luminescence of polycrystalline Ce-doped Y<sub>3</sub>Al<sub>5</sub>O<sub>12</sub> ceramics. *J. Nucl. Mater.* **386–388**, 1049–1051 (2009).
12. Lucchini, M. T., Pauwels, K., Blazek, K., Ochesanu, S. & Auffray, E. Radiation Tolerance of LuAG:Ce and YAG:Ce Crystals under High Levels of Gamma-and Proton-Irradiation. *IEEE Trans. Nucl. Sci.* **63**, 586–590 (2016).
13. Cherepy, N. J. *et al.* Development of transparent ceramic Ce-doped gadolinium garnet gamma spectrometers. *IEEE Trans. Nucl. Sci.* **60**, 2330–2335 (2013).
14. Jarrell, J. T. *et al.* Beta Radiation Hardness of GYGAG(Ce) Transparent Ceramic Scintillators. *IEEE Trans. Nucl. Sci.* **69**, 938–941 (2022).
15. Nikl, M. *et al.* Radiation induced formation of color centers in PbWO<sub>4</sub> single crystals. *J. Appl. Phys.* **82**, 5758–5762 (1997).
16. Han, B., Feng, X., Hu, G., Zhang, Y. & Yin, Z. Annealing effects and radiation damage mechanisms of PbWO<sub>4</sub> single crystals. *J. Appl. Phys.* **86**, 3571–3575 (1999).